Washington University School of Medicine
Digital Commons@Becker

Open Access Publications

2011

Cross-species comparison of orthologous gene expression in human bladder cancer and carcinogen-induced rodent models

Yan Lu
Washington University School of Medicine in St. Louis

Pengyuan Liu
Washington University School of Medicine in St. Louis

Weidong Wen
Washington University School of Medicine in St. Louis

Clinton J. Grubbs
University of Alabama - Birmingham

Reid R. Townsend
Washington University School of Medicine in St. Louis

See next page for additional authors

Follow this and additional works at: http://digitalcommons.wustl.edu/open_access_pubs

Authors

Yan Lu, Pengyuan Liu, Weidong Wen, Clinton J. Grubbs, Reid R. Townsend, James P. Malone, Ronald A. Lubet, and Ming You

Original Article
Cross-species comparison of orthologous gene expression in human bladder cancer and carcinogen-induced rodent models

Yan Lu[1,5], Pengyuan Liu[1,5], Weidong Wen[1], Clinton J Grubbs[2], Reid R Townsend[3], James P. Malone[3], Ronald A Lubet[4], and Ming You[1,6]

[1] Department of Surgery and the Alvin J. Siteman Cancer Center, Washington University School of Medicine, St. Louis, MO 63110, USA; [2]Departments of Surgery, Genetics, and Medicine, University of Alabama at Birmingham, Birmingham, AL 35294, USA; [3]Department of Internal Medicine, Washington University School of Medicine, St. Louis, MO 63110, USA; [4]Chemoprevention Agent Development Research Group, National Cancer Institute, Rockville, MD 20892, USA; [5]Department of Physiology and the Cancer Center, Medical college of Wisconsin, Milwaukee, WI 53226, USA; [6]Department of Pharmacology and Toxicology and the Cancer Center, Medical college of Wisconsin, Milwaukee, WI 53226, USA.

Abstract: Genes differentially expressed by tumor cells represent promising drug targets for anti-cancer therapy. Such candidate genes need to be validated in appropriate animal models. This study examined the suitability of rodent models of bladder cancer in B6D2F1 mice and Fischer-344 rats to model clinical bladder cancer specimens in humans. Using a global gene expression approach cross-species analysis showed that 13~34% of total genes in the genome were differentially expressed between tumor and normal tissues in each of five datasets from humans, rats, and mice. About 20% of these differentially expressed genes overlapped among species, corresponding to 2.6 to 4.8% of total genes in the genome. Several genes were consistently dysregulated in bladder tumors in both humans and rodents. Notably, *CNN1*, *MYL9*, *PDLIM3*, *ITIH5*, *MYH11*, *PCP4* and *FMO5* were found to commonly down-regulated; while *TOP2A*, *CCNB2*, *KIF20A* and *RRM2* were up-regulated. These genes are likely to have conserved functions contributing to bladder carcinogenesis. Gene set enrichment analysis detected a number of molecular pathways commonly activated in both humans and rodent bladder cancer. These pathways affect the cell cycle, HIF-1 and MYC expression, and regulation of apoptosis. We also compared expression changes at mRNA and protein levels in the rat model and identified several genes/proteins exhibiting concordant changes in bladder tumors, including *ANXA1*, *ANXA2*, *CA2*, *KRT14*, *LDHA*, *LGALS4*, *SERPINA1*, *KRT18* and *LDHB*. In general, rodent models of bladder cancer represent the clinical disease to an extent that will allow successful mining of target genes and permit studies on the molecular mechanisms of bladder carcinogenesis.

Keywords: Human bladder cancer, rodent models, gene expression, proteomics, and cross-species comparison.

Introduction

Bladder cancer is one of the most common cancers in the United States, especially in men. In 2009, there will be an estimated 70,980 new cases of bladder cancer with 52,810 cases in males [1]. Approximately 15% of bladder tumors evolve into invasive tumors after infiltration through the basement membrane. Patients with muscle-invasive disease are at high risk for recurrence, progression, and metastasis. Although early stage bladder cancer can be treated surgically, the five-year survival is 45% and 6% for patients with regional and distant recurrences, respectively.

Mice or rats administered *N*-butyl-*N*-(4-hydroxybutyl)-nitrosamine (OH-BBN) develop transitional and squamous cell urinary bladder cancers that have significant histopathological similarities to human bladder cancer and are frequently invasive. These rodent models have been used previously to characterize the tumorigenic process for urinary bladder cancer and to assess the efficacy of potential chemopreventive agents to inhibit the development of blad-

der cancers [2-6]. However, to what degree carcinogen-induced rodent models recapitulate molecular features and biological pathways of human bladder cancer has not been characterized.

Many biological systems operate in an evolutionarily conserved manner across a large number of species. Cross-species analysis of sequence and gene interaction is often applied to determine the function of new genes. In contrast to these static measurements, microarrays measure the dynamic, condition-specific response of complex biological systems. The recent exponential growth in microarray expression datasets allows researchers to combine expression experiments from multiple species to identify genes that are not only conserved in sequence but also regulated in a similar way across species. In this study we performed cross-species analysis of microarray data for human bladder cancer and carcinogen induced rodent bladder cancer. The major objectives of this study were to identify the degree of cross-species overlap on the single-gene level and to determine the similarity of the biological pathways in the cross-species comparison that may be relevant to the mechanism of bladder carcinogenesis. Our analysis demonstrates that cross-species comparisons can be used to obtain important information on gene expression and pathway activation that cannot be obtained when analyzing data from a single species.

Materials and Methods

Rodent models of bladder cancer

Female Fischer-344 rats and male B6D2F1 (C57Bl/6 x DBA/2 F1) mice were obtained from Harlan Sprague-Dawley, Inc. (Indianapolis, IN; virus-free colony 202) at 28 days of age and were housed in polycarbonate cages (five per cage). The animals were kept in a lighted room 12 hours each day and maintained at 22 ± 0.5° C. Teklad 4% mash diet (Harlan Teklad, Madison, WI) and tap water were provided ad *libitum*. In the mouse study, at 56 days of age, animals received the first of 12 weekly gavage treatments with OH-BBN (TCI America, Portland, OR). Each 7.5-mg dose was dissolved in 0.1 ml ethanol: water (25:75). For the rat study, OH-BBN (150 mg/gavage, 2x/week) was started when the rats were 49 days of age and continued for 8 weeks. The carcinogen vehicle was

ethanol:water (20:80) in 0.5 ml. All animals were sacrificed 8 months following the initial OH-BBN treatment.

Bladder tumors were removed and frozen for subsequent molecular assays. All frozen tumor tissues were microdissected to determine the tumor vs normal cell ratio for each specimen. Only microscopic sections from tumor tissues containing more than 80% tumor cells were isolated and stored at -80°C for subsequent RNA isolation. A portion of each tumor was fixed and processed for routine paraffin embedding, cut into 5-μm sections, and mounted for hematoxylin and eosin (H&E) staining. All bladder tumors used in this study were diagnosed as bladder cancers with a mixed histology showing elements of both transitional and squamous cells. Matching normal epithelia came from the same sex and age-matched controls were also microdissected to ensure that specimens consisted of purely normal lung tissue. To isolate bladder epithelia, we separated epithelial cells from the stroma and muscle tissues by cutting the bladder into half and scraping off the epithelium.

Total RNA from normal bladder epithelia and bladder tumors were isolated by Trizol (Invitrogen, Carlsbad, CA) and purified using the RNeasy Mini Kit and RNase-free DNase Set (QIAGEN, Valencia, CA) according to the manufacturer's protocols. *In vitro* transcription-based RNA amplification was then performed on each sample. cDNA for each sample was synthesized using a Superscript cDNA Synthesis Kit (Invitrogen) and a T7-(dT)24 primer, 5′-GGCCAGTGAATTGTAATACGACTCACTA-TAGGGAGGCGG-(dT)24-3′. cDNA were cleaned using phase-lock gels (Fisher cat ID E0032005101) and phenol/chloroform extraction. Then, biotin-labeled cRNA were transcribed *in vitro* from cDNA using a BioArray High Yield RNA Transcript Labeling Kit (ENZO Biochem, New York, NY) and purified again using the RNeasy Mini Kit. The labeled mouse cRNA were applied to Affymetrix MGU74Av2 GeneChips and the labeled rat cRNA were applied to Affymetrix Rat230 2.0 GeneChips or Rat Exon 1.0 ST Array (Affymetrix) according to the manufacturer's recommendations. The raw fluorescence intensity data within CEL files from the platform Affymetrix MGU74Av2 and Rat230 2.0 were preprocessed with Robust Multichip Average (RMA) algorithm [7], as implemented with R packages Affy from Bioconductor (http://

www.bioconductor.org). This algorithm analyzes the microarray data in three steps: a background adjustment, quantile normalization, and finally summation of the probe intensities for each probe set using a log scale linear additive model for the log transform of (background corrected, normalized) PM intensities. Gene-level signal estimates for the CEL files from the platform Rat Exon 1.0 ST Array were derived by quantile sketch normalization using Iterplier algorithm, as implemented with Expression Console v1.1.1 (http://www.affymetrix.com/products_services/software/specific/expression_console_software.affx).

For 1D protein gel electrophoresis, rat samples were solubilized in the following lysis buffers: 25 mM Hepes buffer containing 150 mM NaCl, 10 mM MgCl2, 1% Igepal, 0.25% sodium deoxycholate, 10% glycerol, 2.5 mM EDTA, and protease/phosphatase inhibitors. For 2D protein difference electrophoresis, rat samples were solubilized in 100 μL of lysis buffer (30 mM Tris-Cl, pH 8.5; 7 M urea, 2 M thiourea, 4% CHAPS) containing protease inhibitor cocktail (Roche, Indianapolis, IN) and phosphatase inhibitor cocktails I and II) (Sigma-Aldrich, St. Louis, MO). After centrifugation at 15,000 rpm for 30 min, the supernatant was recovered as cellular protein for the protein expression study. Protein samples from carcinogen-treated and control rats were labeled with DIGE fluorescent dye (GE Healthcare Amersham Biosciences, Piscataway, NJ), and analysis was performed as described previously [8]. A pooled sample consisting of a mixture of small portions of all protein samples obtained was used as internal control. Briefly, after extraction in lysis buffer, three cyanine dyes, Cy2, Cy3, and Cy5 were used to label the protein samples from normal rats, pooled sample, and carcinogen-treated rats, respectively. The same amount of protein were combined and analyzed on the same gel. For the first-dimension separation, the labeling mixture was applied to Immobiline DryStrips (24 cm long, pH 3 to 10; GE Healthcare). The second dimension was carried out with 10-20% SDS-PAGE gels. The Cy2, Cy3, and Cy5-labeled images were subsequently acquired at the recommended wavelengths using a Typhoon 9400 scanner (GE Healthcare). Comprehensive image analysis was performed using DeCyder-2D Differential Analysis Software 5.0 (GE Healthcare). For spot detection and quantification, the differential in-gel analysis (DIA) module of DeCyder was em-

ployed. The biological variance analysis module (BVA) was then used to match the quantified spots of all gels to a chosen master gel. The statistical significance of each expression level was calculated using the Student's *t*-test in the BVA module. Protein expression levels which showed a statistically significant ($p<0.05$) increase or decrease were defined as being significant. In addition to log standardized abundances, the matched spot raw volume data of each sample was used in this analysis. A ratio was created by comparing the raw volume of each protein spot to that of its intra-gel internal standard. Selected gel features were excised and digested *in situ* with trypsin as described previously [8]. The resulting peptide pools were analyzed by tandem mass spectrometry using both MALDI-TOF/TOF instrument (Proteomics 4700, Applied Biosystems, Framingham, MA) and LC-MS/MS (LTQ-FTMS, Thermolectron, San Jose, CA) performed as described [9]. The peptide fragmentation spectra were processed using Data Explorer, v 4.5 and Analyst software (Applied BioSystems, Framingham, MA and Toronto, Ontario). The processed spectra were used to search protein and conceptually-translated database with MASCOT, v 1.9 (Matrix Sciences, London, UK). Precursor error tolerance was set to 100 ppm and MS/MS fragment error tolerance, 0.8 Da. All the proteins identified should have protein scores greater than 40 and individual ions scores greater than 20 with expected value < 0.05. All the MS/MS spectra were further validated manually. When multiple proteins were identified in a single spot, the proteins with the highest number of peptides were considered as those corresponding to the spot.

Human bladder cancer

The expression data for human clinical specimens from two published study were used. Both of these two studies performed gene expression profiles on the Human Genome U133A human GeneChips containing 22,283 probes representing known genes and expression sequence tags (Affymetrix). One dataset is the study of Dyrskjøt et al. [10] including biopsies of normal bladder mucosa from 9 patients without a bladder cancer history, histologically normal mucosa biopsies from 5 cystectomy specimens, biopsies from 28 superficial transitional cell bladder tumors (13 tumors with surrounding carcinoma *in situ* and 15 without surrounding carcinoma *in*

Table 1. Datasets in cross-species gene-expression analysis of bladder cancer

Datasets	No. of normal	No. of tumor	GEO	PubMed
Human_1	14	41	GSE3167	15173019
Human_2	49	109	N/A	16432078
Rat_1	5	5	N/A	17401461
Rat_2*	7	11	N/A	N/A
Mouse	4	4	N/A	15548366

*These are new microarray data from Rat Exon 1.0 ST arrays used for the present study.

situ) and 13 invasive transitional cell carcinomas. The CEL files were downloaded from Gene Expression Omnibus (GEO accession number: GSE3167). The raw fluorescence intensity data within CEL files were preprocessed with RMA algorithm. Another dataset is the study of Sanchez-Carbayo et al. [11], including 49 normal urothelium specimens which were obtained at distant sites from the bladder tumors resected by cystectomy or cystoprostatectomy and 109 bladder cancer (28 superficial and 81 invasive lesions). The expression data of the 157 bladder tissues under study derived by the Affymetrix Microarray Suite 5.0 (MAS 5.0) were included in Supplemental table 10 of the original paper (http://jco.ascopubs.org/cgi/content/full/JCO.2005.03.2375/DC1). Basic information of these five microarray datasets used for cross-species gene-expression analysis of bladder cancer is found in **Table 1**.

Statistical analyses

The probe sets with the average gene expression level of both tumor and normal groups less than 64 derived by MAS 5.0 and Iterplier or less than 6 derived by RMA were excluded in the following statistical analyses. Two-sample student t test was used to identify differentially expressed genes (DEGs) between tumor and normal groups for each dataset. To adjust the multiple testing in the study of high-dimensional microarray data, both tail area-based false discovery rate values (Q values) and local false discovery rate (LFDR) were estimated [12], which was implemented in R package fdrtool (http://www.r-project.org/). The DEGs were defined as genes with Q value < 0.01, LFDR < 0.05 and fold change > 1.5 between two groups.

Gene set enrichment analysis (GSEA) was per-

formed to analyze the pattern of differential gene expression in each dataset respectively. GSEA is a computational method that determines whether a set of genes shows statistically significant differences in expression between two biological states, which has proved successful in discovering molecular pathways involved in human diseases (http://www.broad.mit.edu/gsea). Using the Kolmogorov-Smirnov statistic, GSEA assesses the degree of "enrichment" of a set of genes (e.g. a pathway) in the entire range of the strength of associations with the phenotype of interest. It was used to identify a priori defined sets of genes that were differentially expressed [13, 14]. We used curated gene sets (c2) which contain genes on certain molecular pathways, and GO gene sets (c5) which consist of genes annotated by the same GO terms in the Molecular Signature Database (MSigDB, http://www.broad.mit.edu/gsea/msigdb/msigdb_index.html). For datasets of rodent models, because of small sample size, GSEA with gene permutation option was performed. Selected gene sets identified from GSEA were then visualized with MetaCore™ (http://www.genego.com/).

Quantitative Real-time PCR

Using the samples from rat model of bladder cancer, the relative expressions of eight random selected genes associated with survival were determined by QRT-PCR. RNA was isolated using Trizol reagent per manufacturer's instructions (Invitrogen). One micrograms of total RNA per sample were converted to cDNA using the Im Prom-II RT kit (Promega Co. Madison, WI) for RT-PCR (Invitrogen). Primers for QRT-PCR analysis (**Table 2**) were designed using Primer Express software version 2.0 (Applied Biosystems, Foster City, CA). Amplification of each target DNA was performed with SYBR Green PCR Supermix

Table 2. Oligonucleotide primers and probes used for quantitative real-time PCR Analysis

Gene	Sense primer	Anti-sense primer
GAPDH	GACATGCCGCCTGGAGAA	CTCGGCCGCCTGCTT
ANXA2	GACATTGCCTTCGCCTACCA	ACCAGACAAGGCCGACTTCA
TUBB5	TCCGTTCGCTCAGGTCCTT	CTGCCCCAGACTGACCAAAA
NDN	GGACAGAGTCGCGCTGAAC	TCACATAGATGAGACTCAGGATCATGA
KIF2c	GGAAGGTATTTGATCTGCTCAACAA	CAACCTGCACCTGCTGCTT
KIF22	CCCAGAAATTAAGCCTCTTACAGAA	CCCAGCAAACGTTCCATACTC
CCNA2	ACAGTATGCGGGCCATCCT	AGCCAAATGCAGGGTCTCAT
INHBA	GGCAGGAGGGCCGAAAT	CCTGACTCGGCAAAGGTGAT
E2F8	ACTTTCCCCAAACCACAGGAT	CGACGCCACTGGGATCA

Table 3. Total number and proportion of genes differentially regulated between tumor and normal bladder tissues*

	Up-regulated in tumor		Down-regulated in tumor	
	Number	Proportion (%)	Number	Proportion (%)
Human_1	2729	14.7	2233	12.0
Human_2	3104	24.5	1352	10.7
Rat_1	816	6.5	789	6.3
Rat_2	1069	6.8	1137	7.2
Mouse	514	6.5	621	7.8

*The DEGs were defined as genes with Q value < 0.01, LFDR < 0.05 and fold change > 1.5 between two groups.

(BIO-RAD, Hercules, CA) in BIO-RAD Single Color Real-Time PCR Detection system according to the protocols provided. One microliter of cDNA was added to a 25 mL total volume reaction mixture containing water, SYBR Green PCR SuperMix, and primers. Each real-time assay was done in triplicate on a BioRad MyIQ thermal cycler. Data were collected and analyzed with iQ5 optical system software, version 2.1 software. The internal control gene GAPDH and target genes were amplified with equal efficiencies. The method for assessing if two amplicons have the same efficiency is to look at how ΔC_T ($C_{T,target}$ – $C_{T,GAPDH}$, C_T is cycle number at which the fluorescence signal exceeds background) varies with template dilution. Smaller ΔC_T indicates higher gene expression. The fold change of gene expression in the tumor tissues relative to the normal tissues was calculated as $2^{-\Delta\Delta CT}$ ($\Delta\Delta CT = \Delta C_{T\,tumor}$ – $\Delta C_{T\,normal}$). The differences in expression between two groups were determined by two-tailed Student's t-test. A P-value of less than 0.05 was considered to indicate statistical significance.

Results

Differentially expressed bladder cancer genes in each species

Five microarray datasets were used for cross-species gene-expression analysis of bladder cancer including two human datasets, two rat datasets and one mouse dataset (Table 1). One of two rat datasets is our new microarray data from Rat Exon 1.0 ST arrays. We applied a cut-off of Q value < 0.01, LFDR < 0.05 and fold change > 1.5 to detect genes differentially regulated between tumors and normal bladder tissues in all datasets. Table 3 listed total numbers and proportion of genes differentially regulated between tumor and normal bladder tissues in each dataset. We first randomly chose eight DEGs and evaluated the microarray gene expression results from the cross-species analysis. The relative expression of these candidate bladder cancer genes was determined by QRT-PCR analysis using the samples from the rat model. We confirmed the expression results for
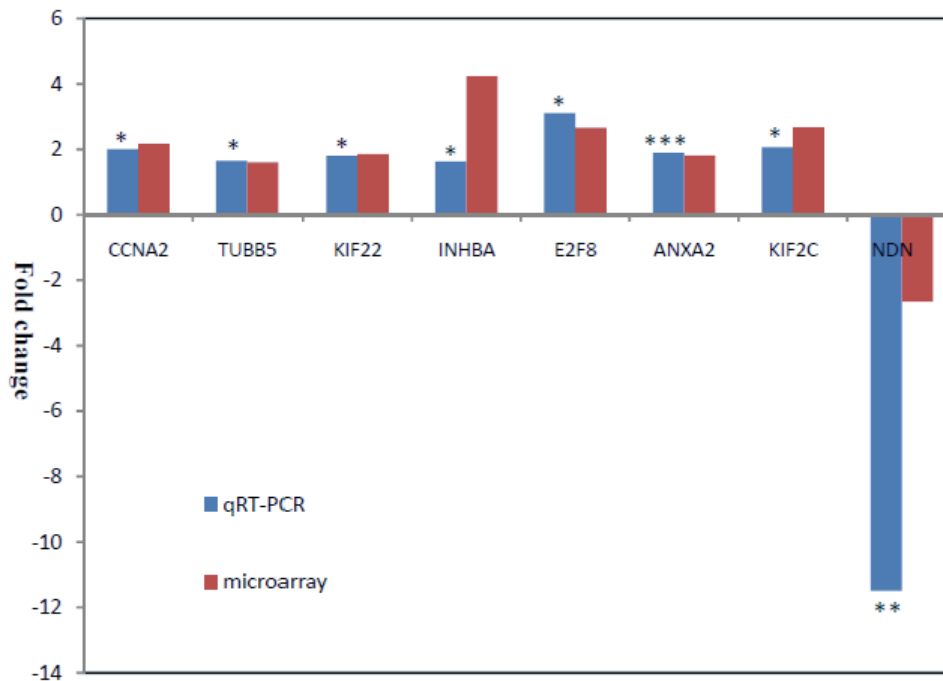
Figure 1. QRT-PCR validation of several candidate bladder cancer genes. Columns represent fold changes for the selected genes with differential expression between normal and tumor samples.. *: P≤0.05; **: P≤0.01; ***: P≤0.005

Table 4. Cross-species overlap of single differentially expressed genes as absolute number or proportion (in brackets) of overlapping orthologous genes between data sets*

	Human_1	Human_2	Rat_1	Rat_2	Mouse
Human_1		891 (10.4%)	165 (2.9%)	177 (2.9%)	154 (3.1%)
Human_2	328 (3.8%)		112 (2.2%)	103 (2.1%)	131 (3.0%)
Rat_1	72 (1.3%)	21 (0.4%)		181 (3.5%)	96 (2.4%)
Rat_2	115 (1.9%)	56 (1.2%)	232 (4.4%)		86 (2.2%)
Mouse	112 (2.2%)	44 (1.0%)	69 (1.7%)	82 (2.1%)	

*Up triangle, up-regulated genes in tumors; down triangle , down-regulated gene in tumors.

all of the eight selected genes (*CCNA2*, *TUBB5*, *KIF22*, *INHBA*, *E2F8*, *ANXA2*, *KIF2C* and *NDN*) (p≤ 0.05) (**Figure 1**). This warrant further investigation and comparison of DEGs among different species.

Approximately, 26 to 34% of genes were identified as DEGs in the two human datasets while only 13 to 14% were in the rodent models. About 14% of DEGs were identified in both human datasets, including 891 up-regulated

genes and 328 down-regulated genes. 7.9% of DEGs were identified in both rat datasets, including 181 up-regulated genes and 232 down-regulated genes. About 20% of these DEGs overlapped among species, corresponding to 2.6 to 4.8% of total genes in the genome (**Table 4**). This suggests that although a large number of genes were identified to be differentially expressed between bladder tumor and normal tissues in each species, most of these genes are not common to the models. These genes

may result from the cancer rather than being causally related.

The top 100 DEGs in each dataset were compared. 91 genes were consistently dysregulated in at least two datasets, including 54 down-regulated genes and 37 up-regulated genes (**Table 5** and **6**). Several genes were consistently dysregulated in bladder tumors in both humans and rodents. These genes are likely to have conserved functions contributing to bladder carcinogenesis. These include, *CNN1* (calponin 1, basic, smooth muscle), *MYL9* (myosin, light chain 9, regulatory), *PDLIM3* (PDZ and LIM domain 3), *ITIH5* (inter-alpha (globulin) inhibitor H5), *MYH11* (myosin, heavy chain 11, smooth muscle), *PCP4* (Purkinje cell protein 4) and *FMO5* (flavin containing monooxygenase 5) which were found to be commonly down-regulated; while *TOP2A* (topoisomerase (DNA) II alpha 170kDa), *CCNB2* (cyclin B2), *KIF20A* (kinesin family member 20A) and *RRM2* (ribonucleotide reductase M2 polypeptide) were found to be commonly up-regulated.

Proteomic analysis

We then evaluated the concordance between gene expression and protein abundance in rodent models of bladder cancer. Ninety-six proteins that were significantly changed between normal and tumor in rat bladder samples were identified using a process of two-dimensional differential gel electrophoresis (2D-DIGE), *in situ* gel digestion, tandem mass spectrometry, and database searching (**Table 7**). Compared with the results from the transcriptomic analyses, 21 genes exhibited concordant changes at the mRNA and protein level in at least one rat mRNA expression dataset (**Table 8**). Among them, *ANXA1* (annexin A1), *ANXA2* (annexin A2), *CA2* (carbonic anhydrase II), *KRT14* (keratin complex 1, acidic, gene 14), *LDHA* (lactate de-hydrogenase A), *LGALS4* (lectin, galactoside-binding, soluble, 4) and *SERPINA1* (serine (or cysteine) proteinase inhibitor, clade A (alpha-1 antiproteinase, antitrypsin), member 1) were increased in both rat gene expression datasets and concordant changes were observed at the protein level. *KRT18* and *LDHB* were decreased in both rat datasets and showed concordant changes at the protein level (**Table 9**). The remainder did not show significant differences in gene expression, or showed discordant changes. These results suggest that many pro-

teins which are changed in tumor might involve post-translational modification and the expression changes cannot be observed at the transcriptional level.

Molecular pathways identified by gene enrichment analysis (GSEA)

GSEA was performed using the curated gene sets to identify molecular pathways involved in bladder carcinogenesis. A false discovery rate (FDR) of ≤ 0.25 was used for defining GSEA enriched gene sets [13, 14]. Using the curated gene sets c2, GSEA detected 74 enriched gene sets in bladder tumors in all of the five datasets from three different species (**Table 10**). These pathways include cell cycle, HIF-1 (hypoxia-inducible factor 1) and MYC pathways which were activated in bladder tumors. GSEA also detected additional 14 enriched gene sets among all of the five datasets using the curated gene sets c5 (**Table 10**). Several pathways are particularly interesting, including apoptosis, and the mitotic (M) phase of the cell cycle (**Figure 2** and **3**). Dysregulated genes are significantly over-represented in these pathways during bladder neoplastic transformation and progression in both humans and rodents.

Discussion

Rodent models represent a powerful tool in the research of cancer mechanisms, prevention and therapy. Determination of the extent as to which findings in animal models can be translated to human disease is an important step. In this study we examined whether global gene expression profiling can assist in determining the suitability of rodent models of bladder cancer for the detection of cancer-related genes and prediction of cancer prevention effects.

The present study found that rodent models of bladder cancer (in OH-BBN treated B6D2F1 mice and Fischer-344 rats) accurately represent the clinical situation to an extent that will allow successful mining of target genes. About 20% of DEGs in bladder tumors overlapped among species, corresponding to 2.6 to 4.8% of total genes in the genome. Several genes that were concordantly regulated across species are of particular interest. Among these genes is ribonucleotide reductase M2 polypeptide (RRM2) which was increased in tumors across three species. RRM2 is an enzyme that catalyzes the

Table 5. Down-regulated genes observed in at least two datasets*

Genes	Description	Datasets
CASQ2	calsequestrin 2 (cardiac muscle)	human1, human2
DES	desmin	human1, human2
DMD	dystrophin (muscular dystrophy, Duchenne and Becker types)	human1, human2
DMN	desmuslin	human1, human2
FHL1	four and a half LIM domains 1	human1, human2
FOXF1	forkhead box F1	human1, human2
KIAA0367	KIAA0367	human1, human2
LMOD1	leiomodin 1 (smooth muscle)	human1, human2
PLN	phospholamban	human1, human2
PTGIS	prostaglandin I2 (prostacyclin) synthase	human1, human2
REEP1	receptor accessory protein 1	human1, human2
SORBS1	sorbin and SH3 domain containing 1	human1, human2
TNS1	tensin 1	human1, human2
TPM2	tropomyosin 2 (beta)	human1, human2
CNN1	calponin 1, basic, smooth muscle	human1, human2, mouse
MYL9	myosin, light chain 9, regulatory	human1, human2, mouse
PDLIM3	PDZ and LIM domain 3	human1, human2, mouse
ITIH5	inter-alpha (globulin) inhibitor H5	human1, mouse
MYH11	myosin, heavy chain 11, smooth muscle	human2, mouse
PCP4	Purkinje cell protein 4	human2, mouse
FMO5	flavin containing monooxygenase 5	rat1, mouse
ACE2	angiotensin I converting enzyme (peptidyl-dipeptidase A) 2	rat1, rat2
AHRR	aryl-hydrocarbon receptor repressor	rat1, rat2
CAPN13	calpain 13	rat1, rat2
CASKIN1	CASK interacting protein 1	rat1, rat2
CYP11A1	cytochrome P450, family 11, subfamily A, polypeptide 1	rat1, rat2
CYP1A1	cytochrome P450, family 1, subfamily A, polypeptide 1	rat1, rat2
CYP3A18	cytochrome P450, family 3, subfamily A, polypeptide 18	rat1, rat2
DPYD	dihydropyrimidine dehydrogenase	rat1, rat2
EGFL6	EGF-like-domain, multiple 6	rat1, rat2
FNDC5	fibronectin type III domain containing 5	rat1, rat2
HSD11B2	hydroxysteroid (11-beta) dehydrogenase 2	rat1, rat2
HTR4	5-hydroxytryptamine (serotonin) receptor 4	rat1, rat2
IGF2BP3	insulin-like growth factor 2 mRNA binding protein 3	rat1, rat2
PAK3	p21 (CDKN1A)-activated kinase 3	rat1, rat2
PCBP3	poly(rC) binding protein 3	rat1, rat2
PLAG1	pleiomorphic adenoma gene 1	rat1, rat2
PLCE1	phospholipase C, epsilon 1	rat1, rat2
PRKCQ	protein kinase C, theta	rat1, rat2
RPS6KA2	ribosomal protein S6 kinase, 90kDa, polypeptide 2	rat1, rat2
SHANK2	SH3 and multiple ankyrin repeat domains 2	rat1, rat2
SLC15A2	solute carrier family 15 (H+/peptide transporter), member 2	rat1, rat2
SLC23A1	solute carrier family 23 (nucleobase transporters), member 1	rat1, rat2
TRPV4	transient receptor potential cation channel, subfamily V, member 4	rat1, rat2
TSHR	thyroid stimulating hormone receptor	rat1, rat2
KRT20	keratin 20	rat1, rat2, mouse
HSD17B2	hydroxysteroid (17-beta) dehydrogenase 2	rat1, rat2, mouse
SH3GL2	SH3-domain GRB2-like 2	rat1, rat2, mouse
SLC16A7	solute carrier family 16, member 7 (monocarboxylic acid transporter 2)	rat1, rat2, mouse
FLJ45455 (RGD1564618)	FLJ45455 protein (similar to novel protein)	rat2, human2
HIP1R	huntingtin interacting protein 1 related	rat2, mouse
NDRG2	NDRG family member 2	rat2, mouse
UPK2	uroplakin 2	rat2, mouse
MFSD4	major facilitator superfamily domain containing 4	rat2, mouse

* The DEGs were defined as genes with Q value < 0.01, LFDR < 0.05 and fold change > 1.5 between two groups; the top 100 DEGs in each dataset were compared.

Table 6. Up-regulated genes observed in at least two datasets*

Genes	Description	Datasets
CDH1	cadherin 1, type 1, E-cadherin (epithelial)	human1, human2
EIF2AK1	eukaryotic translation initiation factor 2-alpha kinase 1	human1, human2
KPNA2	karyopherin alpha 2 (RAG cohort 1, importin alpha 1)	human1, human2
KRT7	keratin 7	human1, human2
LSR	lipolysis stimulated lipoprotein receptor	human1, human2
MLF1IP	MLF1 interacting protein	human1, human2
PRC1	protein regulator of cytokinesis 1	human1, human2
SLC38A1	solute carrier family 38, member 1	human1, human2
SPINT1	serine peptidase inhibitor, Kunitz type 1	human1, human2
TH1L	TH1-like (Drosophila)	human1, human2
TOP2A	topoisomerase (DNA) II alpha 170kDa	human1, human2, mouse
CCNB2	cyclin B2	rat1, human1
KIF20A	kinesin family member 20A	rat1, human1
RRM2	ribonucleotide reductase M2 polypeptide	rat1, human1, mouse
CEACAM1	carcinoembryonic antigen-related cell adhesion molecule 1 (biliary glycoprotein)	rat1, mouse
CTGF	connective tissue growth factor	rat1, mouse
MMP7	matrix metallopeptidase 7 (matrilysin, uterine)	rat1, mouse
S100A9	S100 calcium binding protein A9	rat1, mouse
SERPINB2	serpin peptidase inhibitor, clade B (ovalbumin), member 2	rat1, mouse
DDIT4	DNA-damage-inducible transcript 4	rat1, rat2
KCNN4	potassium intermediate/small conductance calcium-activated channel, subfamily N, member 4	rat1, rat2
MALL	mal, T-cell differentiation protein-like	rat1, rat2
MMP3	matrix metallopeptidase 3 (stromelysin 1, progelatinase)	rat1, rat2
PROM1	prominin 1	rat1, rat2
RGD1563692		rat1, rat2
TNFRSF12A	tumor necrosis factor receptor superfamily, member 12A	rat1, rat2
TRPV2	transient receptor potential cation channel, subfamily V, member 2	rat1, rat2
TSPAN1	tetraspanin 1	rat1, rat2
VWA1	von Willebrand factor A domain containing 1	rat1, rat2
VWF	von Willebrand factor	rat1, rat2
WIF1	WNT inhibitory factor 1	rat1, rat2
FGFBP1	fibroblast growth factor binding protein 1	rat1, rat2, mouse
GPX2	glutathione peroxidase 2 (gastrointestinal)	rat1, rat2, mouse
MMP12	matrix metallopeptidase 12 (macrophage elastase)	rat1, rat2, mouse
ANXA8	annexin A8	rat2, mouse
BHLHB2	basic helix-loop-helix domain containing, class B, 2	rat2, mouse
MMP13	matrix metallopeptidase 13 (collagenase 3)	rat2, mouse

* The DEGs were defined as genes with Q value < 0.01, LFDR < 0.05 and fold change > 1.5 between two groups; the top 100 DEGs in each dataset were compared.

formation of deoxyribonucleotides from ribonucleotides [15]. Deoxyribonucleotides in turn are used in the synthesis of DNA. The reaction catalyzed by RRM2 is strictly conserved in all living organisms [16]. Furthermore RRM2 plays a critical role in regulating the total rate of DNA synthesis so that DNA to cell mass is maintained at a constant ratio during cell division and DNA repair [17]. RRM2 plays an important role in tumor angiogenesis and growth through regula-

tion of the expression of TSP-1 and VEGF [18]. TOP2A was consistently increased across datasets and encodes a DNA topoisomerase, an enzyme that controls and alters the topologic states of DNA during transcription. TOP2A plays an important role in checkpoint activation and the maintenance of genomic stability [19]. Increased TOP2A correlated with advanced histological grading, microvascular invasion, and an early age onset of the hepatocellular

Table 7. Protein changed signficantly between rat tumors and normal bladder tissues

Gene Symbol	Protein Name	Gene Bank gi	Fold
AK2	adenylate kinase 2	13591872	-2.5
AK3	adenylate kinase 3	6978479	3.2
AKR1A1	aldo-keto reductase family 1, member A1	13591894	6.2
ALB	Albumin	55391508	4.6
ALDH2	mitochondrial aldehyde dehydrogenase precursor	45737868	-5.8
ALDH3A1	aldehyde dehyrogenase family 3, member A1	47482124	4.6
ALDH3B1	fatty aldehyde dehydrogenase-like	55742838	-3.8
ANXA1	Lipocortin I [Rattus sp.]	235879	3.4
ANXA2	Calpactin I heavy chain	312253	7.1
APOA4	Apolipoprotein A-IV	60552712	-3.5
BANF1	barrier to autointegration factor 1	16758438	4.9
CA2	Ca2 protein (carbonic anhydrase)	41388872	3.4
CA3	carbonic anhydrase 3	31377484	-5.5
CACYBP	calcyclin binding protein	51948388	-2.5
CCT2	chaperonin containing TCP1, subunit 2 (beta)	54400730	4.0
CCT4	chaperonin delta subunit	33149357	8.5
CKB	creatine kinase	203474	4.9
CNN1	calponin	313818	3.0
DCTN2	dynactin 2	51948450	-4.3
DES	desmin	38197676	-2.2
DYNC1LI2	lumican	13591983	4.2
ENTPD5	ectonucleoside triphosphate dephosphorylase	40786479	-13.1
FAM65B	Liver-regeneration-related protein LRRG069 (Ab2-162)	33086566	-9.5
GC	vitamin D binding protein prepeptide	203927	3.8
GDA	guanine deaminase	7533042	3.8
GSTA4	similar to GST 8 (8-8)	27720723	4.2
GSTA5	glutathione-S-transferase, alpha type2	51036637	9.9
GSTM5	glutathione transferase (EC 2.5.1.18)	204501	4.0
GSTP1	GST pi2	25453412	5.4
HIBCH	3-hydroxyisobutyryl-Coenzyme A hydrolase (predicted)	61556993	6.2
HSPB1	heat shock protein 27	204665	3.4
KA11	type I keratin KA11	57012432	4.2
KRT10	keratin 10	57012436	1.3
KRT13	keratin 13	51591909	4.3
KRT14	keratin complex 1, acidic, gene 14 (predicted)	56912233	4.4
KRT15	type I keratin KA15	51591903	-1.8
KRT16	type I keratin KA16	56847618	-2.0
KRT18	keratin complex 1, acidic, gene 18	60688216	-18.9
KRT19	keratin complex 1, acidic, gene 19	42409519	-12.6
KRT20	keratin 20	27465585	5.9
KRT4	type II keratin Kb4	57012360	7.6
KRT5	type II keratin 5 [Mus musculus]	16303309	5.7
KRT7	similar to keratin complex 2 (predicted)	34868200	-5.1
KRT73	type II keratin Kb36	57012358	-5.0
KRT8	cytokeratin-8 [Rattus sp.]	30352203	-10.6
LDHA	lactate dehydrogenase A	8393706	3.3
LDHB	lactate dehydrogenase B	6981146	-3.5
LGALS4	lectin, galactoside-binding, soluble, 4 (galectin 4)	6981152	4.3
LZIC	leucine zipper and CTNNBIP1 domain containing	61557405	9.8
MDH2	malate dehydrogenase, mitochondrial	42476181	4.0
MYL9	myosin regulatory light chain, isoform C [Rattus sp.]	998522	5.0
NAGA	N-acetyl galactosaminidase, alpha (predicted)	58865810	5.9
NIT1	Nit 1 protein	56268926	-2.4
NME2	RBL-NDP kinase 18kDa subunit (p18)	206580	8.0
NQO2	NAD(P)H dehydrogenase, quinone 2	51948400	2.4
PA2G4	proliferation associated 2G4, 38kDa	51948384	6.0

PDIA6	CaBP1	488838	-7.7
PDLIM1	LIM protein	8393153	3.9
PECR	peroxisomal trans-2-enoyl-CoA reductase	18959236	4.3
PGRMC1	progesterone receptor membrane component 1	11120720	3.7
PKLR	L-type pyruvate kinase	297533	4.2
PKM2	Unnamed protein product	56929	4.2
PPM1F	protein phosphatase 1F (PP2C domain containing)	28461153	5.9
PPP1R7	Protein phosphatase 1, regulatory (inhibitor) subunit 7	57032943	-34.9
PRDX2	peroxiredoxin 2	8394432	8.0
PRELP	proline arginine-rich end leucine-rich repeat protein	16758116	8.5
PRKCDBP	protein kinase C, delta binding protein	19745164	-3.5
PROSC	similar to Proline synthetase associated(predicted)	62662820	-6.1
PSMC4	proteasome 26S ATPase subunit 4	25742677	-3.9
PTGR1	Leukotriene B4 12-hydroxydehydrogenase	59809128	8.1
PZP	alpha-1-macroglobulin	202857	-3.5
RPSA	laminin receptor 1	8393693	-4.3
RUVBL1	RuvB-like protein 1	22208848	4.0
RUVBL2	RuvB-like 2	70794778	-15.7
S100A4	S100 A4 (calvasculin)	6981326	5.3
S100A6	S100 calcium binding protein A6 (calcyclin)	16758986	4.9
SAE1	Ubiquitin-like 1 (sentrin) activating enzyme E1A	50925905	-3.5
SELENBP1	selenium binding protein 2	18266692	4.0
SERPINA1	serine protease inhibitor alpha 1	51036655	2.5
SERPINH1	serpinh 1 protein	55824765	4.6
SNCG	synuclein, gamma [Mus musculus]	6755592	-3.2
STRAP	serine/threonine kinase receptor associated protein	4063383	-18.5
TALDO1	transaldolase	12002054	4.1
TCAG7.1260	aldoketoreductase family 1	27465603	8.8
TGM2	transglutaminase 2, C polypeptide	42476287	5.1
TKT	transketolase	1729977	6.0
TPM1	tropomyosin alpha isoform	14134104	4.0
TUBA1C	tubulin, alpha 6 (predicted)	58865558	-2.8
TXN	thioredoxin	16758644	10.4
UBE2V2	Ubiquitin-conjugating enzyme E2 variant 2	24817674	4.3
UCHL1	ubiquitin carboxy-terminal hydrolase L1	61098212	3.4
VDAC1	voltage dependent anion channel	4105605	6.5
VIM	vimentin	57480	4.1
YARS	Yars predicted protein	68534287	6.0
YWHAE	Tyrosine 3-monooxygenase	30583161	-3.8

Table 8. Genes exhibited concordant changes at both gene expression and protein levels

	mRNA expression arrays*						Protein expression arrays†		
Symbol	Gene Name	probe_set	Fold	Q-value	LFDR	Dataset	Protein Name	Gene Bank gi	Fold
Anxa1	annexin A1	1367614_at	12.3	3.2E-05	3.6E-05	Rat1	Lipocortin I [Rattus sp.]	235879	3.4
Anxa2	annexin A2	1367584_at	2.7	5.2E-04	7.9E-04	Rat1	Calpactin I heavy chain	312253	7.1
Car2	carbonic anhydrase II	1367733_at	3.4	1.4E-03	2.7E-03	Rat1	Ca2 protein (carbonic anhydrase)	41388872	3.4
Car2	carbonic anhydrase II	1386922_at	3.1	2.5E-03	6.4E-03	Rat1	Ca2 protein (carbonic anhydrase)	41388872	3.4
Gda	guanine deaminase	1387659_at	3.1	2.0E-03	4.3E-03	Rat1	guanine deaminase	7533042	3.8
Krt14	keratin 14	1371895_at	22.5	3.0E-05	3.6E-05	Rat1	keratin complex 1, acidic, gene 14 (predicted)	56912233	4.4
Krt18	keratin 18	1388155_at	-4.0	3.4E-03	7.9E-03	Rat1	keratin complex 1, acidic, gene 18	60688216	-18.9
Krt5	keratin 5	1370863_at	2.6	2.8E-03	6.6E-03	Rat1	type II keratin 5 [Mus musculus]	16303309	5.7
Ldha	lactate dehydrogenase A	1367586_at	2.8	7.9E-04	1.4E-03	Rat1	lactate dehydrogenase A	8393706	3.3
Ldhb	lactate dehydrogenase B	1370218_at	-2.1	2.6E-03	6.6E-03	Rat1	lactate dehydrogenase B	6981146	-3.5
Lgals4	lectin, galactoside-binding, soluble, 4	1368269_at	12.7	3.5E-03	7.9E-03	Rat1	lectin, galactoside-binding, soluble, 4 (galectin 4)	6981152	4.3
Nit1	nitrilase 1	1398049_at	-1.5	3.5E-03	7.9E-03	Rat1	Nit 1 protein	56268926	-2.4
S100a4	S100 calcium-binding protein A4	1367846_at	2.6	1.6E-04	2.0E-04	Rat1	S100 A4 (calvasculin)	6981326	5.3
Serpinh1	serine (or cysteine) peptidase inhibitor, clade H, member 1	1371310_s_at	4.1	3.1E-03	6.6E-03	Rat1	serinh 1 protein	55824765	4.6
Vim	vimentin	1367574_at	2.6	6.9E-03	1.8E-02	Rat1	vimentin	57480	4.1
Anxa1	annexin A1	7060990	5.7	4.3E-07	1.6E-06	Rat2	Lipocortin I [Rattus sp.]	235879	3.4
Anxa2	annexin A2	7337587	1.8	2.6E-05	1.4E-04	Rat2	Calpactin I heavy chain	312253	7.1
Banf1	barrier to autointegration factor 1	7059728	1.8	4.6E-03	1.9E-02	Rat2	barrier to autointegration factor 1	16758438	4.9
Car2	carbonic anhydrase II	7206103	3.5	5.0E-04	2.3E-03	Rat2	Ca2 protein (carbonic anhydrase)	41388872	3.4
Ka11	type I keratin KA11	7082629	11.1	1.9E-09	3.5E-09	Rat2	type I keratin KA11	57012432	4.2
Krt14	keratin 14	7082623	11.1	1.4E-09	3.4E-09	Rat2	keratin complex 1, acidic, gene 14 (predicted)	56912233	4.4
Krt18	keratin 18	7191382	-4.7	2.3E-06	9.5E-06	Rat2	keratin complex 1, acidic, gene 18	60688216	-18.9
Ldha	lactate dehydrogenase A	7031732	2.6	7.0E-05	3.1E-04	Rat2	lactate dehydrogenase A	8393706	3.3
Ldhb	lactate dehydrogenase B	7270937	-2.4	2.1E-07	5.3E-07	Rat2	lactate dehydrogenase B	6981146	-3.5
Lgals4	lectin, galactoside-binding, soluble, 4	7030215	16.0	1.5E-03	7.4E-03	Rat2	lectin, galactoside-binding, soluble, 4 (galectin 4)	6981152	4.3
Nme2	non-metastatic cells 2, protein (NM23B) expressed in	7081660	1.8	2.0E-03	8.7E-03	Rat2	RBL-NDP kinase 18kDa subunit (p18)	206580	8
Prosc	proline synthetase co-transcribed homolog (bacterial)	7152637	-1.7	3.5E-06	1.4E-05	Rat2	similar to Proline synthetase associated(predicted)	62662820	-6.1
Serpina1	serine (or cysteine) proteinase inhibitor, clade A (alpha-1 antiproteinase, antitrypsin), member 1	7309988	5.8	9.7E-03	4.0E-02	Rat2	serine protease inhibitor alpha 1	51036655	2.5
Txn1	thioredoxin 1	7286798	1.5	1.8E-03	8.0E-03	Rat2	thioredoxin	16758644	10.4
Vdac1	voltage-dependent anion channel 1	7067512	1.9	7.2E-03	2.9E-02	Rat2	voltage dependent anion channel	4105605	6.5

* The DEGs were defined as genes with Q value < 0.01, LFDR < 0.05 and fold change > 1.5 between two groups.
† Protein expression levels which showed a statistically significant (p<0.05) increase or decrease in tumors as compared with their matched normal bladder.

Table 9. Genes exhibited concordant changes at both mRNA expression and protein levels at both rat bladder cancer datasets

Gene	mRNA (Rat_1)				mRNA (Rat_2)				Protein	
	probe_set	Normal	Tumor	Fold	probe_set	Normal	Tumor	Fold	Protein Name	Fold
Anxa1	1367614_at	9.0	12.6	12.3	7060990	1106.1	6285.0	5.7	Lipocortin I [Rattus sp.]	3.4
Anxa2	1367584_at	10.9	12.3	2.7	7337587	3077.4	5579.3	1.8	Calpactin I heavy chain	7.1
Krt14	1371895_at	8.2	12.7	22.5	7082623	633.3	7004.7	11.1	keratin complex 1, acidic, gene 14	4.4
Ldha	1367586_at	9.8	11.3	2.8	7031732	641.3	1646.2	2.6	lactate dehydrogenase A	3.3
Lgals4	1368269_at	6.8	10.5	12.7	7030215	135.2	2162.5	16.0	lectin, galactoside-binding, soluble, 4	4.3
Serpinh1	1371310_s_at	7.3	9.3	4.1	7309988	33.4	194.2	5.8	serine protease inhibitor alpha 1	2.5
Krt18	1388155_at	12.3	10.3	-4.0	7191382	626.6	133.0	-4.7	keratin complex 1, acidic, gene 18	-18.9
Ldhb	1370218_at	11.4	10.4	-2.1	7270937	2438.2	1010.8	-2.4	lactate dehydrogenase B	-3.5

Table 10. Molecular pathways identified by gene enrichment analysis in all five datasets

Gene sets	Rat_1		Rat_2		Mouse		Human_1		Human_2	
	Size	FDR	Size	FDR	Size	FDR	Size	FDR	Size	FDR
The curated gene sets c2										
ADIP_DIFF_CLUSTER4	32	0.012	24	0.000	18	0.006	32	8E-06	32	1E-04
ADIP_DIFF_CLUSTER5	33	0.039	32	3E-05	16	0.007	35	0.000	35	8E-06
BASSO_REGULATORY_HUBS	105	0.235	103	0.020	77	0.043	138	0.036	138	0.000
BENNETT_SLE_UP	20	7E-05	19	0.010	17	0.001	28	0.021	28	0.009
BRCA_ER_NEG	583	0.002	655	2E-05	494	0.000	867	0.003	867	0.001
BRCA_PROGNOSIS_NEG	62	0.001	62	0.008	41	0.001	94	4E-05	94	0.000
BRENTANI_CELL_CYCLE	65	0.182	58	6E-05	49	0.005	80	3E-04	80	0.002
CANCER_NEOPLASTIC_META_UP	53	0.088	40	0.084	37	0.028	60	0.000	60	0.000
CANCER_UNDIFFERENTIATED_META_UP	59	0.003	41	3E-05	37	0.000	67	0.000	67	0.000
CANTHARIDIN_DN	35	0.042	32	0.018	30	0.071	49	4E-04	49	0.000
CELL_CYCLE	53	0.225	51	7E-05	45	0.002	74	0.000	74	0.000
CELL_CYCLE_KEGG	58	0.222	58	4E-04	48	0.002	80	0.000	80	8E-06
CHANG_SERUM_RESPONSE_UP	108	0.241	107	0.013	92	0.013	143	0.002	143	0.000
CMV_ALL_UP	73	0.239	68	0.057	59	0.154	90	0.167	90	0.006
CMV_IE86_UP	34	0.072	38	0.003	26	0.088	49	0.000	49	0.000
CROMER_HYPOPHARYNGEAL_MET_VS_NON_DN	53	0.222	52	4E-04	42	0.003	80	0.020	80	0.000
CROONQUIST_IL6_STARVE_UP	27	0.011	24	4E-05	20	2E-04	33	0.000	33	8E-06
DER_IFNA_UP	40	0.010	44	0.074	37	0.019	65	0.042	65	0.001
DER_IFNB_UP	64	0.047	63	0.184	55	0.063	91	0.139	91	0.001
DNA_REPLICATION_REACTOME	38	0.012	29	7E-05	24	0.132	44	0.000	44	0.000
DOX_RESIST_GASTRIC_UP	25	0.043	28	1E-04	15	0.001	43	0.000	43	0.000
GAY_YY1_DN	212	0.004	193	1E-04	154	0.001	220	7E-06	220	0.051
GREENBAUM_E2A_UP	29	0.001	27	3E-05	22	2E-04	32	0.000	32	1E-05
HCC_SURVIVAL_GOOD_VS_POOR_DN	85	0.065	89	0.021	78	0.026	121	4E-04	121	0.000
HESS_HOXAANMEIS1_DN	61	0.222	46	0.006	41	0.051	55	0.093	55	0.004
HESS_HOXAANMEIS1_UP	61	0.234	46	0.005	41	0.061	55	0.087	55	0.003
HG_PROGERIA_DN	19	0.095	20	4E-04	16	0.005	25	3E-04	25	0.012
HIF1_TARGETS	31	0.030	29	0.001	31	0.003	35	0.021	35	0.005
HOFFMANN_BIVSBII_BI_TABLE2	226	0.037	150	4E-05	117	0.001	184	7E-06	184	2E-05
HOFMANN_MDS_CD34_LOW_AND_HIGH_RISK	21	0.204	30	0.018	26	0.004	46	0.042	46	0.017
HSA03050_PROTEASOME	22	0.236	20	0.007	19	0.135	22	0.002	22	0.000
HSA04110_CELL_CYCLE	82	0.210	79	3E-04	70	0.001	102	0.000	102	0.000
HSA04115_P53_SIGNALING_PATHWAY	47	0.217	43	0.002	39	0.002	62	0.020	62	3E-04
IDX_TSA_UP_CLUSTER3	78	3E-04	66	0.000	42	0.000	83	0.000	83	0.000
IFN_ALPHA_UP	26	0.100	28	0.214	24	0.027	40	0.239	40	0.020
IFNA_HCMV_6HRS_UP	33	0.001	32	0.191	25	0.002	53	0.011	53	0.030

IFNALPHA_HCC_UP	23	0.012	18	0.157	23	0.005	29	0.047	29	0.005
IFNALPHA_NL_UP	18	0.018	17	0.218	18	0.012	27	0.013	27	0.002
INOS_ALL_UP	45	0.177	40	0.036	35	0.159	52	0.005	52	0.000
KENNY_WNT_UP	34	0.046	34	0.200	29	0.025	46	0.129	46	0.005
LE_MYELIN_UP	105	0.000	63	0.000	50	0.002	82	3E-05	82	0.000
LEE_MYC_E2F1_UP	42	0.001	44	0.122	38	3E-04	55	0.015	55	0.051
LEE_TCELLS2_UP	587	0.082	669	0.005	489	0.011	939	0.037	939	0.004
LEE_TCELLS3_UP	53	0.010	63	3E-05	34	3E-04	93	0.000	93	1E-05
LEI_MYB_REGULATED_GENES	239	0.032	234	0.023	200	0.001	317	0.057	317	0.000
LI_FETAL_VS_WT_KIDNEY_DN	114	0.051	106	0.003	85	0.001	159	0.000	159	0.000
MYC_ONCOGENIC_SIGNATURE	105	0.217	123	0.096	96	0.062	173	0.021	173	0.005
MYC_TARGETS	38	0.222	34	0.001	37	0.010	39	0.104	39	0.003
OLDAGE_DN	38	0.040	33	2E-05	29	0.001	47	0.000	47	0.000
P21_ANY_DN	26	0.004	27	0.002	22	0.008	32	0.000	32	2E-04
POD1_KO_UP	256	0.166	282	0.070	210	2E-04	339	0.011	339	0.037
PRMT5_KD_UP	158	0.082	130	0.013	99	4E-04	166	0.007	166	0.000
PROTEASOME	17	0.095	15	0.021	16	0.115	17	1E-04	17	2E-05
PROTEASOME_DEGRADATION	29	0.192	20	0.019	27	0.213	31	0.015	31	9E-06
RADAEVA_IFNA_UP	33	0.004	32	0.147	37	0.001	50	0.003	50	0.001
RADIATION_SENSITIVITY	19	0.075	19	0.095	19	0.046	24	0.063	24	0.005
SANA_IFNG_ENDOTHELIAL_UP	34	0.020	43	0.004	31	0.000	60	0.161	60	0.196
SCHUMACHER_MYC_UP	43	0.081	35	0.020	31	0.023	50	0.002	50	0.000
SERUM_FIBROBLAST_CELLCYCLE	83	1E-04	90	0.000	53	0.000	110	0.000	110	0.000
SERUM_FIBROBLAST_CORE_UP	123	0.132	138	0.010	105	0.049	174	2E-04	174	0.000
SHEPARD_BMYB_MORPHOLINO_DN	128	0.023	129	0.010	99	0.009	152	4E-05	152	0.020
SHEPARD_CRASH_AND_BURN_MUT_VS_WT_DN	100	0.120	109	0.115	81	0.056	137	8E-05	137	0.011
SHEPARD_GENES_COMMON_BW_CB_MO	48	0.004	49	0.072	37	0.064	60	0.000	60	0.008
SHIPP_FL_VS_DLBCL_DN	29	0.103	27	0.190	28	0.056	34	3E-05	34	0.000
STEMCELL_EMBRYONIC_UP	1162	0.189	909	0.083	717	0.075	1165	0.050	1165	0.000
TARTE_PLASMA_BLASTIC	244	0.038	221	5E-05	198	0.001	305	0.000	305	0.000
UVB_NHEK3_ALL	316	0.084	280	0.001	279	0.004	390	0.237	390	0.000
UVB_NHEK4_6HRS_UP	21	0.157	19	0.075	19	0.043	27	0.067	27	0.001
VANTVEER_BREAST_OUTCOME_GOOD_VS_POOR_DN	51	0.001	45	0.006	37	0.002	63	4E-05	63	0.001
WIELAND_HEPATITIS_B_INDUCED	63	0.000	66	0.018	60	3E-05	106	0.001	106	0.050
YU_CMYC_UP	43	0.000	28	0.003	20	0.002	27	0.000	27	0.000
ZELLER_MYC_UP	23	0.047	19	0.014	23	0.057	23	0.030	23	0.001
ZHAN_MMPC_SIMAL	36	0.239	37	0.011	34	0.008	47	0.071	47	0.011
ZUCCHI_EPITHELIAL_UP	30	0.095	30	0.072	30	3E-04	41	0.034	41	5E-04

The curated gene sets c5

APOPTOSIS_GO	307	0.136	322	0.003	269	0.062	380	0.131	380	0.020
CELL_CYCLE_PHASE	115	0.217	121	0.002	83	0.018	145	0.000	145	0.009

CELL_CYCLE_PROCESS	133	0.209	136	0.002	94	0.025	165	0.000	165	0.001
INTERPHASE	49	0.232	43	0.056	35	0.174	58	0.011	58	0.006
M_PHASE	74	0.181	83	0.002	53	0.006	95	0.000	95	0.081
M_PHASE_OF_MITOTIC_CELL_CYCLE	54	0.178	61	9E-05	42	0.001	70	0.000	70	0.007
MITOSIS	52	0.129	60	1E-04	42	0.001	67	0.000	67	0.009
MITOTIC_CELL_CYCLE	102	0.141	110	0.002	78	0.019	128	0.000	128	3E-04
PROGRAMMED_CELL_DEATH	307	0.141	323	0.003	270	0.059	381	0.131	381	0.017
PROTEOLYSIS	121	0.178	138	0.116	117	0.003	162	0.246	162	0.078
REGULATION_OF_APOPTOSIS	245	0.161	255	0.004	213	0.050	300	0.082	300	0.029
REGULATION_OF_DNA_METABOLIC_PROCESS	33	0.134	34	0.001	20	0.217	38	0.130	38	0.115
REGULATION_OF_MITOSIS	30	0.137	28	4E-04	20	0.016	35	0.000	35	0.049
REGULATION_OF_PROGRAMMED_CELL_DEATH	245	0.172	256	0.004	214	0.046	301	0.078	301	0.023
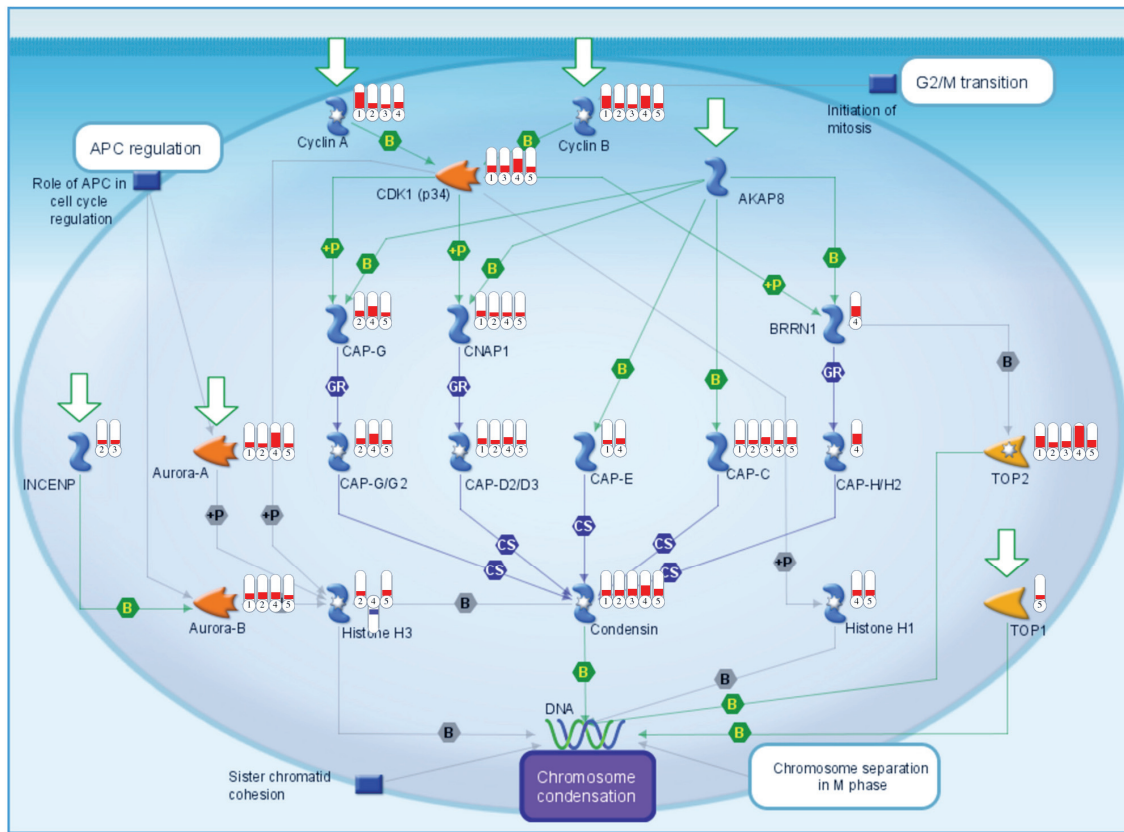
Figure 2. Cell cycle genes consistently altered across species during bladder carcinogenesis. Red and blue indicates overexpressed and underexpressed genes in tumor samples, respectively. 1, dataset Rat_1; 2, Rat_2; 3, Mouse; 4, Human_1; and 5, Human_2.

malignancy [20]. TOP2A has been reported to be over-expressed in pancreatic adenocarcinoma [21], renal medullary carcinomas [22], ovarian cancer [23], acute lymphocytic leukemia [24], colorectal cancer [25], gastric carcinoma [26] and laryngeal squamous cell carcinoma [27]. CCNB2 (Cyclin B2), found commonly upregulated, is a member of the cyclin family, specifically the B-type cyclins. Cyclin B2 also binds to transforming growth factor beta RII and thus cyclin B2/cdc2 may play a key role in transforming growth factor beta-mediated cell cycle control [28]. These commonly regulated genes across mouse, rat and human may be functionally important regulators of bladder tumorigenesis.

To integrate the expression changes observed in multiple datasets we utilized pathway analysis algorithms to identify functional classifications that were altered in bladder tumors com-

pared to normal bladder epithelium of mouse, rat and human. Biological processes and molecular functions that were enriched in tumors included apoptosis, cell cycle, and DNA replication. In particular, TOP2A was consistently activated in the biological classification of regulation of programmed cell death. Several genes including CCNB2, KIF20A and TOP2A have previously been reported to be up-regulated in bladder carcinogenesis [29]. CCNB2 was also found to be up-regulated in the cell cycle. Additional pathways enriched in bladder tumors included those for interphase and proteolysis. Our data suggest that human bladder cancer and carcinogen-induced rodent models may show more common similarity at global cellular pathway levels than at the single-gene levels previously described.

The proportion of dysregulated orthologous genes overlapped in two species is low which
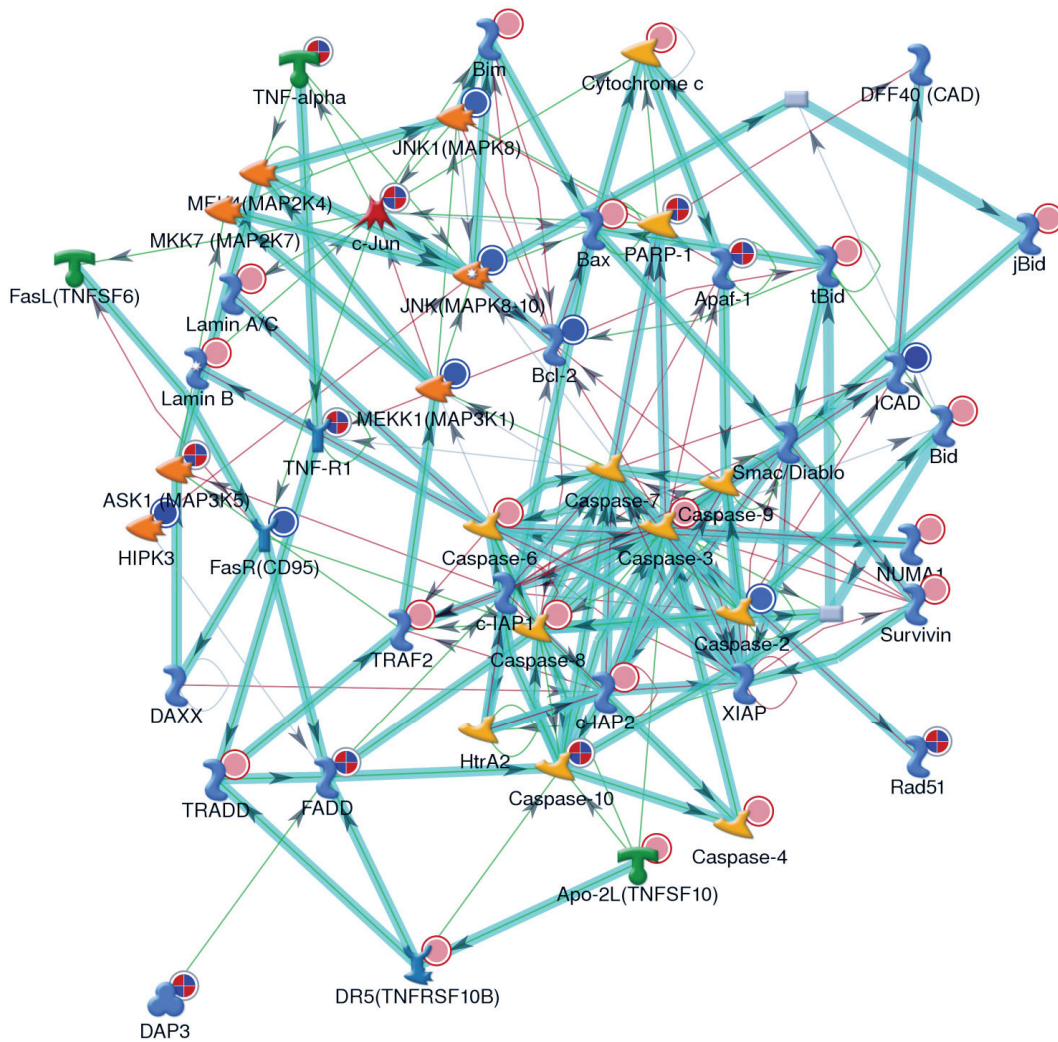
Figure 3. Network analyses of apoptosis, programmed cell death and cell death. Multiple genes in this network are dysregulated in bladder tumors. Red and blue indicates overexpressed and underexpressed genes in tumor samples, respectively.

may be partly explained by the histological difference in bladder cancer among mouse, rat and human. Histopathology of B6D2F1 mouse bladder cancers have previously shown that these urinary bladder carcinomas had either transitional cell differentiation alone or in combination with either squamous or glandular differentiation or both squamous and glandular differentiation [2]. These patterns were also observed in highly invasive variants of human transitional cell bladder carcinoma [30]. Immunohistochemical staining of intermediate filament types showed that OH-BBN-induced rat

bladder tumors had marked quantitative and qualitative differences from the most common, purely transitional, human bladder carcinomas [31]. Smaller lesions were similar to human urothelial dysplasia both histologically and immunohistochemically. Progression of the lesions demonstrated large exophytic papillomas with extensive endophytic epithelial growth into abundant stroma and these lesions showed increasing predominance of squamous over transitional elements. Immunohistochemical findings confirmed these results and also demonstrated that morphologically indistinct cells,

even in early lesions, express heavier cytokeratins characteristic of keratinizing squamous epithelium [30, 31]. The proportion of invasive transitional cell carcinomas in human bladder cancer biopsies from Sanchez-Carbayo et al. (81/108) is much higher than that from Dyrskjøt et al. (13/41) [10] and this may explain why there was more gene expression overlap between the rodent models and human bladder cancer from Sanchez-Carbayo et al. than those from Dyrskjøt et al. (4.1-4.8% vs. 2.6-4.0%). These data also suggest that histology information should be taken into account when analyzing animal models of bladder cancer.

Acknowledgments

Please address correspondence to: Ming You, MD, PhD, Department of Pharmacology and Toxicology and the Cancer Center, Medical college of Wisconsin, Milwaukee, WI 53226, USA. Tel: 414-955-2565 Fax: 414-955-6058, E-mail: myou@mcw.edu

References

[1] Jemal A, Siegel R, Ward E, Hao Y, Xu J and Thun MJ. Cancer Statistics, 2009. CA Cancer J Clin 2009; caac.20006.

[2] Becci PJ, Thompson HJ, Strum JM, Brown CC, Sporn MB and Moon RC. N-Butyl-N-(4-Hydroxybutyl)nitrosamine-induced Urinary Bladder Cancer in C57BL/6 x DBA/2 F1 Mice as a Useful Model for Study of Chemoprevention of Cancer with Retinoids. Cancer Res 1981; 41: 927-932.

[3] Grubbs CJ, Lubet RA, Koki AT, Leahy KM, Masferrer JL, Steele VE, Kelloff GJ, Hill DL and Seibert K. Celecoxib Inhibits N-Butyl-N-(4-hydroxybutyl)-nitrosamine-induced Urinary Bladder Cancers in Male B6D2F1 Mice and Female Fischer-344 Rats. Cancer Res 2000; 60: 5599-5602.

[4] Grubbs CJ, Moon RC, Squire RA, Farrow GM, Stinson SF, Goodman DG, Brown CC and Sporn MB. 13-cis-Retinoic acid: inhibition of bladder carcinogenesis induced in rats by N-butyl-N-(4-hydroxybutyl)nitrosamine. Science 1977; 198: 743-744.

[5] McCormick DL, Ronan SS, Becci PJ and Moon RC. Influence of total dose and dose schedule on induction of urinary bladder cancer in the mouse by N-butyl-N-(4-hydroxy-butyl)nitrosamine. Carcinogenesis 1981; 2: 251-254.

[6] Moon RC, Kelloff GJ, Detrisac CJ, Steele VE, Thomas CF and Sigman CC. Chemoprevention of OH-BBN-induced bladder cancer in mice by piroxicam. Carcinogenesis 1993; 14: 1487-1489.

[7] Irizarry RA, Bolstad BM, Collin F, Cope LM, Hobbs B and Speed TP. Summaries of Affymetrix GeneChip probe level data. Nucleic Acids Res 2003; 31: e15.

[8] Bredemeyer AJ, Lewis RM, Malone JP, Davis AE, Gross J, Townsend RR and Ley TJ. A proteomic approach for the discovery of protease substrates. Proc Natl Acad Sci U S A 2004; 101: 11785-11790.

[9] King JB, Gross J, Lovly CM, Rohrs H, Piwnica-Worms H and Townsend RR. Accurate mass-driven analysis for the characterization of protein phosphorylation. Study of the human Chk2 protein kinase. Anal Chem 2006; 78: 2171-2181.

[10] Dyrskjot L, Kruhoffer M, Thykjaer T, Marcussen N, Jensen JL, Moller K and Orntoft TF. Gene expression in the urinary bladder: a common carcinoma in situ gene expression signature exists disregarding histopathological classification. Cancer Res 2004; 64: 4040-4048.

[11] Sanchez-Carbayo M, Socci ND, Lozano J, Saint F and Cordon-Cardo C. Defining molecular profiles of poor outcome in patients with invasive bladder cancer using oligonucleotide microarrays. J Clin Oncol 2006; 24: 778-789.

[12] Strimmer K. A unified approach to false discovery rate estimation. BMC Bioinformatics 2008; 9: 303.

[13] Mootha VK, Lindgren CM, Eriksson KF, Subramanian A, Sihag S, Lehar J, Puigserver P, Carlsson E, Ridderstrale M, Laurila E, Houstis N, Daly MJ, Patterson N, Mesirov JP, Golub TR, Tamayo P, Spiegelman B, Lander ES, Hirschhorn JN, Altshuler D and Groop LC. PGC-1alpha-responsive genes involved in oxidative phosphorylation are coordinately downregulated in human diabetes. Nat Genet 2003; 34: 267-273.

[14] Subramanian A, Tamayo P, Mootha VK, Mukherjee S, Ebert BL, Gillette MA, Paulovich A, Pomeroy SL, Golub TR, Lander ES and Mesirov JP. Gene set enrichment analysis: a knowledge-based approach for interpreting genome-wide expression profiles. Proc Natl Acad Sci U S A 2005; 102: 15545-15550.

[15] Elledge SJ, Zhou Z and Allen JB. Ribonucleotide reductase: regulation, regulation, regulation. Trends Biochem Sci 1992; 17: 119-123.

[16] Torrents E, Aloy P, Gibert I and Rodriguez-Trelles F. Ribonucleotide reductases: divergent evolution of an ancient enzyme. J Mol Evol 2002; 55: 138-152.

[17] Herrick J and Sclavi B. Ribonucleotide reductase and the regulation of DNA replication: an old story and an ancient heritage. Mol Microbiol 2007; 63: 22-34.

[18] Zhang K, Hu S, Wu J, Chen L, Lu J, Wang X, Liu X,

Zhou B and Yen Y. Overexpression of RRM2 decreases thrombspondin-1 and increases VEGF production in human cancer cells in vitro and in vivo: implication of RRM2 in angiogenesis. Mol Cancer 2009; 8: 11.

[19] Luo K, Yuan J, Chen J and Lou Z. Topoisomerase IIalpha controls the decatenation checkpoint. Nat Cell Biol 2009; 11: 204-210.

[20] Wong N, Yeo W, Wong WL, Wong NL, Chan KY, Mo FK, Koh J, Chan SL, Chan AT, Lai PB, Ching AK, Tong JH, Ng HK, Johnson PJ and To KF. TOP2A overexpression in hepatocellular carcinoma correlates with early age onset, shorter patients survival and chemoresistance. Int J Cancer 2009; 124: 644-652.

[21] Baiocchi GL, Villanacci V, Rossi E, Gheza F, Portolani N and Giulini SM. HER-2/neu and topoisomerase-II-alpha expression and genic amplification in pancreatic adenocarcinoma. Dig Dis Sci 2009; 54: 2049-2051.

[22] Albadine R, Wang W, Brownlee NA, Toubaji A, Billis A, Argani P, Epstein JI, Garvin AJ, Cousi R, Schaeffer EM, Pavlovich C and Netto GJ. Topoisomerase II alpha status in renal medullary carcinoma: immuno-expression and gene copy alterations of a potential target of therapy. J Urol 2009; 182: 735-740.

[23] Faggad A, Darb-Esfahani S, Wirtz R, Sinn B, Sehouli J, Konsgen D, Lage H, Weichert W, Noske A, Budczies J, Muller BM, Buckendahl AC, Roske A, Eldin Elwali N, Dietel M and Denkert C. Topoisomerase IIalpha mRNA and protein expression in ovarian carcinoma: correlation with clinicopathological factors and prognosis. Mod Pathol 2009; 22: 579-588.

[24] Wang YH, Takanashi M, Tsuji K, Tanaka N, Shiseki M, Mori N and Motoji T. Level of DNA topoisomerase IIalpha mRNA predicts the treatment response of relapsed acute leukemic patients. Leuk Res 2009; 33: 902-907.

[25] Coss A, Tosetto M, Fox EJ, Sapetto-Rebow B, Gorman S, Kennedy BN, Lloyd AT, Hyland JM, O'Donoghue DP, Sheahan K, Leahy DT, Mulcahy HE and O'Sullivan JN. Increased topoisomerase IIalpha expression in colorectal cancer is associated with advanced disease and chemotherapeutic resistance via inhibition of apoptosis. Cancer Lett 2009; 276: 228-238.

[26] Liang Z, Zeng X, Gao J, Wu S, Wang P, Shi X, Zhang J and Liu T. Analysis of EGFR, HER2, and TOP2A gene status and chromosomal polysomy in gastric adenocarcinoma from Chinese patients. BMC Cancer 2008; 8: 363.

[27] Shvero J, Koren R, Shvili I, Yaniv E, Sadov R and Hadar T. Expression of human DNA Topoisomerase II-alpha in squamous cell carcinoma of the larynx and its correlation with clinicopathologic variables. Am J Clin Pathol 2008; 130: 934-939.

[28] Bellanger S, de Gramont A and Sobczak-Thepot J. Cyclin B2 suppresses mitotic failure and DNA re-replication in human somatic cells knocked down for both cyclins B1 and B2. Oncogene 2007; 26: 7175-7184.

[29] Yu D, Cozma D, Park A and Thomas-Tikhonenko A. Functional validation of genes implicated in lymphomagenesis: an in vivo selection assay using a Myc-induced B-cell tumor. Ann N Y Acad Sci 2005; 1059: 145-159.

[30] Koss LG. Tumors of the urinary bladder. In: Firminger HI, editors. Atlas of Tumor Pathology. Washington, DC: Armed Forces Institute of Pathology; 1975. p.

[31] Herman CJ, Vegt PD, Debruyne FM, Vooijs GP and Ramaekers FC. Squamous and transitional elements in rat bladder carcinomas induced by N-butyl-N-4-hydroxybutyl-nitrosamine (BBN). A study of cytokeratin expression. Am J Pathol 1985; 120: 419-426.